J Electr Eng Technol.2018; 13(1): 501-512
http://doi.org/10.5370/JEET.2017.13.1.501

ISSN(Print) 1975-0102
ISSN(Online) 2093-7423

A Self-Powered RFID Sensor Tag for Long-Term Temperature Monitoring in Substation

Zhongbin Chen*, Fangming Deng†, Yigang He, Zhen Liang***, Zhihui Fu* and Chaolong Zhang§**

Abstract – Radio frequency identification (RFID) sensor tag provides several advantages including battery-less operation and low cost, which are suitable for long-term monitoring. This paper presents a self-powered RFID temperature sensor tag for online temperature monitoring in substation. The proposed sensor tag is used to measure and process the temperature of high voltage equipments in substation, and then wireless deliver the data. The proposed temperature sensor employs a novel phased-locked loop (PLL)-based architecture and can convert the temperature sensor in frequency domain without a reference clock, which can significantly improve the temperature accuracy. A two-stage rectifier adopts a series of auxiliary floating rectifier to boost its gate voltage for higher power conversion efficiency. The sensor tag chip was fabricated in TSMC 0.18μm 1P6M CMOS process. The measurement results show that the proposed temperature sensor tag achieve a resolution of 0.15 °C /LSB and a temperature error of -0.6/0.7 °C within the range from -30 °C to 70 °C. The proposed sensor tag achieves maximum communication distance of 11.8 m.

Keywords: High voltage equipment, Temperature monitoring, Radio Frequency Identification (RFID), Reliability

1. Introduction

The operating states of high voltage equipments in transformer substation significantly influence the stability and reliability of power grid [1]. Due to the oxidation in the long running process, resistance of heating points of all the high voltage equipments above becomes larger, which results in intensively local temperature increasing. The high temperature resulted from overheating accelerates the oxidization process of the metal in the contact, thus forming a vicious circle [2]. Generally, numerous serious accidents such as electric arc conflagration and explosion are all resulted from quickly local temperature rising, which would cause great financial loss and protracted power outage. So, it is of great importance to on-line monitoring the temperature of high voltage equipments in substation [3, 4].

As for smart grid, a widely distributed, reliable and maintenance-free monitoring system is essential for its reliable operation [5, 6]. Traditional off-line temperature monitoring method for high voltage equipments in substation always rely on human and infrared thermometer for regular inspection [7]. However, these methods cannot monitor the change of temperature or the real time temperature of the heating points, which decreases its popularities. Moreover, the high costs for the implementation and human resources further limit it being widely employed. There are several online monitoring methods that are proposed to solve the abovementioned problems. Temperature sensor mounted on conductive arm of the high voltage switch cabinet is presented to online monitoring the temperature [8]. But this device has big volume, which is not convenient for implementation. What's more, the high running costs for using battery as power supply further restrict the wide application of this technology. Optical fiber temperature measurement technology [9] is introduced to online monitoring the temperature of high voltage equipments. It has precise measurement results and excellent performance of electrical insulation. Nevertheless, the fiber is vulnerable to the harsh environment, besides, the high costs for implementation and maintenance decreases its popularity. In addition, the location of the sensor is not introduced in this paper.

The past few years has witnessed a rapid development in wireless sensor networks (WSN), which has been widely employed for both industrial and medical applications due to its high flexibility and fast deployment [10-19]. However, WSN have drawbacks of high power consumption, large size, and high costs. Besides, it cannot identify the sensor location by conventional WSN. Recently, Radio Frequency Identification (RFID) technology has been widely employed

† Corresponding Author: Dept. of Electrical and Automation Engineering, East China Jiaotong University, China. (dengfangming@ecjtu.jx.cn)
* Dept. of Electrical and Automation Engineering, East China Jiaotong University, China.
** Dept. of Electrical Engineering and Automation, Hefei University of Technology, China.
*** Rising Micro Electronics Co., Ltd., China.
§ Dept. of Physics and Electronic Engineering, Anqing Normal University, China.
Received: December 11, 2016; Accepted: August 18, 2017

in logistics, traffic management, and food production [20-22], but the simple identification functionality limits it being widely adopted. Daniel. *et al* introduced the sensor-augmented RFID tags, which integrate the functions of sensing, data processing, storage and data transmission into the passive RFID tags. This has raised great interests from both industrial and academia. But the maximum communication distance of this kind of sensor tag is only 5m, which is far less than the safely accessible distance. Battery-assisted RFID sensor tag has an operating distance exceeds 18m, but battery increases the cost [23]. Thus, the self-powered RFID sensor tag is proposed for long-term, long-range, and large scale application [24]. It can realize online monitoring and has a sensing range longer than 20m. Moreover, the self-powered RFID sensor tag doesn't need regular change of battery, which decreases the cost and maintenance pressure. In [25, 26] radio frequency energy relay is introduced. The introduced relay can obtain the electric field energy and wirelessly power the RFID sensor tags around, which guarantees the reliable performance of the proposed RFID sensor tag.

This paper presents a novel RFID sensor tag for long-term and long-range temperature monitoring in substation (<220 kV). To our knowledge, this is the first work to monitor the heating points' temperature by using self-powered RFID sensor tag. Compared with the traditional temperature measurement, the proposed sensor tag can automatically measure the temperature in a wireless way. Furthermore, the sensor tag can work without a battery for low-cost and long-term real-time monitoring application. The rest of the paper is organized as follows. Section 2 presents the overall architecture of the proposed sensor tag and the whole temperature monitoring system. Section 3 analyzes the design of the self-powered temperature sensor tag. Section 4 illustrates the measurement results and compared it with the results of traditional measurement. The conclusion is made in section 5.

2. System design

915 MHz communication frequency is the nature choice for the self-powered RFID sensor tag due to its good anti-electromagnetic interference (EMI) performance. In order to avoid the interference on communication, we finally choose the 433MHz as the power transmitting frequency [24].

2.1 Substation temperature monitoring system

Fig. 1 illustrates the whole system of the relay networks, consisting of RFID sensor tags and energy relays [26]. Energy relays are used to harvest energy from electric fields and radiate RF energy to power the RFID sensor tags around, which are incorporated with various sensors to monitor the environment. In this way, the autonomous

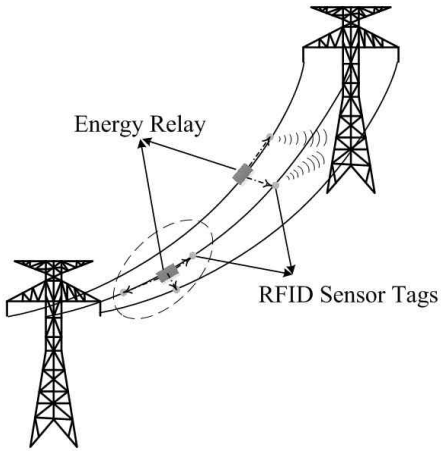

Fig. 1. Energy relay network

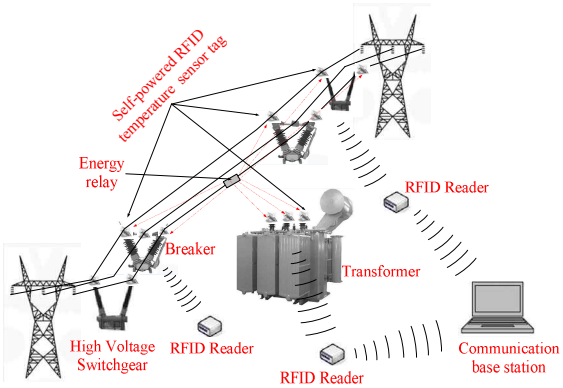

Fig. 2. The overall substation temperature monitoring system

temperature monitoring can be realized. Moreover, the use of energy relay can further realize the sustainable operation of the proposed self-powered RFID temperature sensor tag.

The power received by the RFID sensor tags can be expressed as:

$$P_r = \frac{P_e G_e G_t \lambda^2}{(4\pi)^2 d^2 L} \quad (1)$$

where P_e is the radiated power from the energy relay, G_e is the antenna gain of the energy relay, λ is the wavelength of the electromagnetic wave, d is the distance between the energy relay and the sensor tag, and L is the loss of hardware which is independent with the transmission process.

Fig. 2 shows the overall substation temperature monitoring system, which consists of energy relays [26], self-powered RFID temperature sensor tag, RFID reader, and communication base station. The self-powered RFID temperature sensor tag is employed to acquire the temperature and location of heating points of high voltage equipments. Then, the information of temperature and location is wirelessly transmitted to the RFID reader. Both the self-powered RFID temperature sensor tag and the

RFID reader are compatible with EPC Generation-2 UHF protocol. The RFID reader transmits the collected data to the communication base station which is part of the SCADA (Supervisory Control and Data Acquisition) system. The SCADA system will analyze the accumulated data, if the measured temperature is abnormal, it will send instructions to handle it.

2.2 Architecture of the proposed temperature sensor tag

The theoretical practicable operating power of an RFID tag P_t is calculated from the Friis transmission equation [20]:

$$P_t = E_r \cdot G_a \cdot \eta_r \cdot \left(\frac{\lambda}{4\pi d}\right)^2 \tag{2}$$

where E_r is the effective isotropic radiation power of a reader, G_a is the tag antenna gain, η_r is the RF-to-DC power conversion efficiency of the rectifier, λ is the wavelength of the electromagnetic wave and d is the communication distance. From Eq. (1), the communication distance d can be expressed as:

$$d = \frac{\lambda}{4\pi}\sqrt{\frac{E_r \cdot G_a \cdot \eta_r}{P_t}} \tag{3}$$

Hence in order to achieve longer communication distance, lower P_t and higher η_r are critical for the design of UHF RFID tag, for E_r is limited by regional regulations (4 W is the maximum transmitted power on UHF band in USA) and G_a is roughly determined by the allowable antenna area (1.64 for the $\lambda/2$ dipole antenna). Sensitivity is a parameter to characterize the RFID performance. Since the antenna and the sensor tag both have a crucial influence on the sensitivity, the sensor tag and antenna should be taken into consideration jointly. The theoretical sensitivity can be calculated by the following equation:

$$S_{tag} = P_{on} G_a \left(\frac{\lambda}{4\pi d}\right)\eta_p \tag{4}$$

where P_{on} represents the minimum equivalent radiated power required to communicate with the sensor tag, and η_p is the polarization loss factor due to the circularly polarized antenna of measurement equipment.

Fig. 3 shows the architecture of the proposed self-powered temperature sensor tag based on EPC Generation-2 UHF communication protocol. Except the antenna and matching network, the blocks including rectifier, regulator, demodulator/modulator, POR, clock generator, digital baseband, electrically erasable programmable read-only memory (EEPROM) and sensors, are fabricated in a single chip for low-cost application. The energy harvesting antenna receives the electromagnetic waves from energy relay and the matching network ensures the optimal point of power matching between the antenna and the tag chip. The UHF RFID antenna receives instructions from RFID reader and sends the required data back to the reader. The rectifier and regulator blocks convert the received RF signal into stable voltages to energize the sensor tag, and demodulates (modulates) the received (transmitted) signal. The clock generator and power on reset (POR) blocks provide the clock and reset signals for digital parts and sensor interface respectively. The digital baseband decodes the demodulated signal and executes the received commands. Furthermore, the digital baseband generates the encoded data for modulation and controls the on-chip sensors. The EEPROM is designed to store the information such as EPC code, security information and sensing data.

3. Key Blocks Design

3.1 Temperature sensor

The proposed temperature sensor employs a Phase-Locked Loop (PLL)-based architecture and digitalizes the sensor signal in frequency domain without a reference

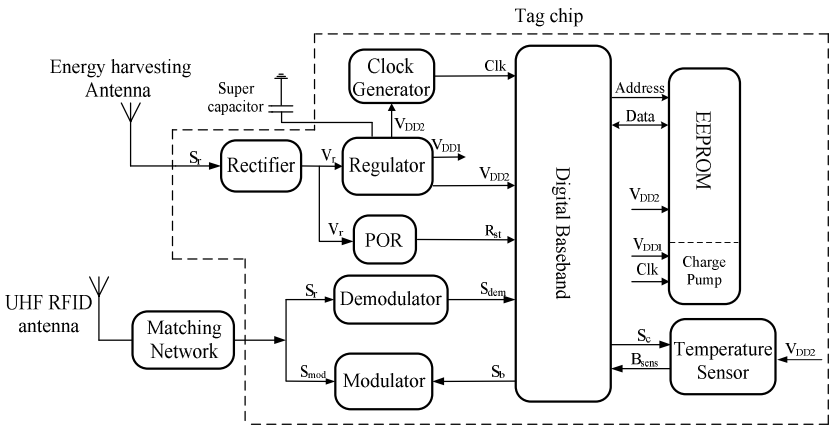

Fig. 3. Architecture of the proposed RFID temperature sensor tag

clock [27]. As shown in Fig. 4, this sensor consists of a Temperature-Controlled Oscillator (TCO), a Digitally-Controlled Oscillator (DCO) and a 1-bit Phase Detector (PD). Both the TCO and the DCO are implemented as N-stage inverter-based ring oscillators. Assuming an equal rise and fall time for the different stages respectively, the oscillating frequency f_{osc} of the ring oscillator can be expressed as follows:

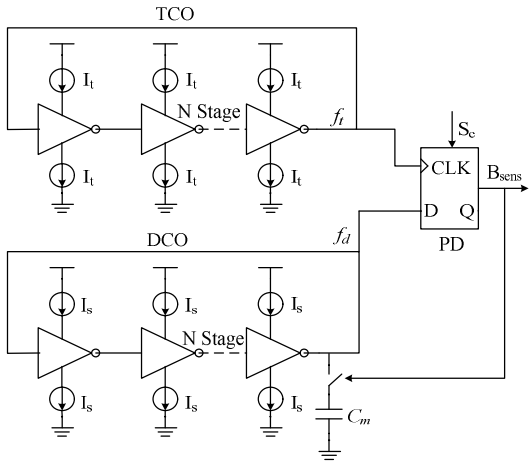

Fig. 4. Proposed temperature sensor

$$f_{osc} = \frac{1}{t_d} = \frac{I_l}{V_m C_l} \tag{5}$$

where t_d is the delay time of the loop, I_l is the current flowing through the inverter, C_l is the total output capacitor of the loop, and V_m is the swing range of the output voltage which mostly equals to the supply voltage V_{DD}. According to this equation, if the current source of the TCO I_t is a Proportional To Absolute Temperature (PTAT) current, the oscillating frequency of the TCO f_t is a PTAT frequency.

The PD measures whether the output frequency of the TCO f_t leads or lags the output frequency of the DCO f_d, and hence the DCO is only steered by a 1-bit signal B_{sens}. When the entire feedback loop is locked, f_d shifts between a maximum and minimum value (f_{max} and f_{min}) which correspond to the maximal and minimal value of the temperature. The average value of f_d will equal f_t. Therefore, the output of PD B_{sens} represents the digital value of the temperature information.

3.2 Rectifier

There are several proposed techniques aimed to decrease the turn on voltage, including using Schottky diodes [28,

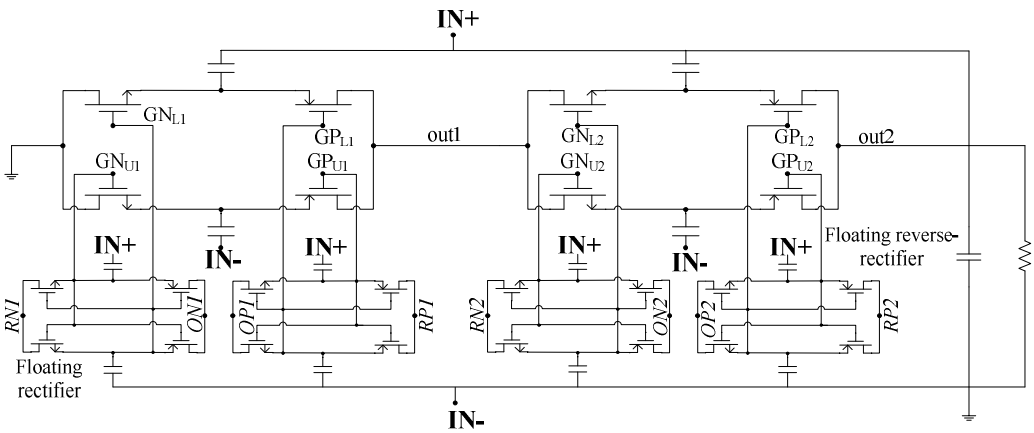

Fig. 5. Schematic of the proposed rectifier

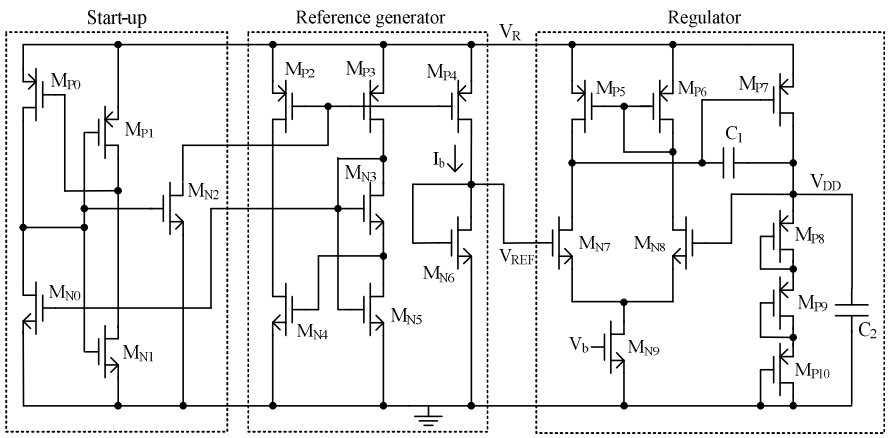

Fig. 6. Schematic of the proposed voltage regulator

29] and applying low threshold voltage transistors [30], requiring additional cost of advanced CMOS processing. The proposed rectifier adopts two-stage architecture and each stage takes the same circuit design (shown in Fig. 5) to ensure enough large supply voltage (>0.8 V). We take the second stage as example to analyze how this proposed rectifier works. The output of first stage (out1) works as the reference for the floating rectifier (RN2) and the output of the second stage (out2) works as the reference for the floating reverse-rectifier (RP2). The boosted gate drive voltages $GN_{L2,U2}$ and $GP_{L2,U2}$ are generated by the two floating rectifiers, and they are the shifted versions of the RF voltages $M_{U2,L2}$, meeting the following conditions [29]:

$$GN_{L2} > M_{L2}, GN_{U2} > M_{U2}, GP_{L2} < M_{L2}, GP_{U2} < M_{U2} \quad (6)$$

The floating rectifier (ON2) output has a higher DC value with respect to out2, it does not drive any load while out2 drives are succeeding stage. So, the intermediate node voltage of the floating rectifier ($GN_{L2,U2}$) has a higher DC value relative to ($M_{U2,L2}$). The floating reverse-rectifier is also redesigned to ensure the DC component of its intermediate node voltages ($GP_{L2,U2}$) is smaller than that of the main rectifier ($GN_{L2,U2}$) [31] all the time.

3.3 Regulator

Due to the large variation of the output voltage of rectifier, a reference circuit with small supply voltage coefficient is necessary to generate a stable reference voltage. The traditional way to generate stable 1.25V reference voltage is using a band gap reference circuit [32]. However it cannot meet the low-voltage requirement of low-power application. Fig. 6 shows the schematic of the proposed voltage regulator. It is implemented in standard CMOS process without a band gap reference and consists of three parts. The transistors M_{P0}-M_{P1} and M_{N0}-M_{N2} compose a start-up block, which is added as a precautionary measure to ensure bias in the desired state. The transistors M_{P2}-M_{P4} and M_{N3}-M_{N6} compose a reference generator block to provide a reference voltage V_{REF} of 0.26 V which is compensated by temperature and supply voltage. The transistors M_{P5}-M_{P10} and M_{N7}-M_{N9} compose a regulator to generate a stable voltage V_{DD} of 1.0 V for other circuits.

The reference generator works with all the MOSFETs in the subthreshold region without resistors. Current sources are composed of three NMOS transistors M_{N3}-M_{N5} and the current mirror is composed of M_{P2}-M_{P4}. The reference generator can be simplified by a current source I_b and a diode-connected NMOS M_{N6} shown in Fig. 7.

While $V_{DS} \geq 4V_T$, the output voltage of reference generator can be expressed as [33]:

$$V_{REF} = V_{GS} = V_{th} + mV_T \ln\left\{\frac{I_b}{(W/L)C_{ox}\mu V_T^2}\right\} \quad (7)$$

where V_{DS} is the drain-to-source voltage, V_T is the thermal voltage, V_{th} is MOSFET threshold voltage, m is the subthreshold slope parameter, W/L represents the transistor aspect ratio, C_{ox} is the gate oxide capacitance per unit area, μ is the electron mobility, V_{GS} is the gate-to-source voltage.

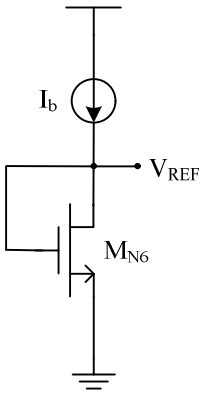

Fig. 7. Simplified reference generator

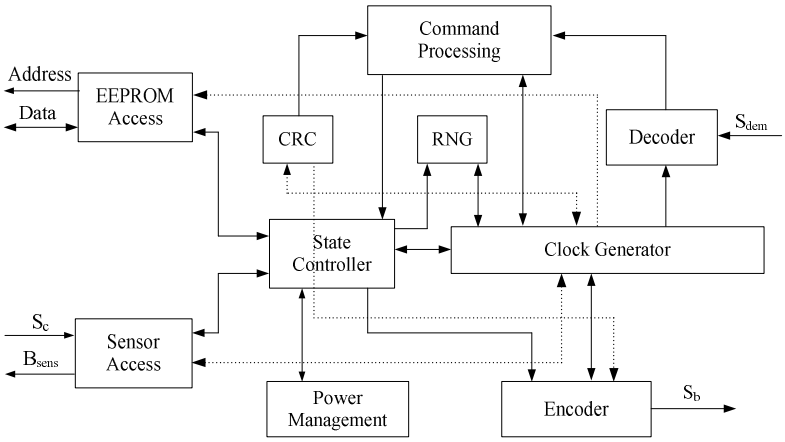

Fig. 8. Block diagram of the proposed digital baseband

3.4 Digital Baseband

Fig. 8 shows the architecture of the proposed digital baseband which is fully compatible with EPC Generation-2 UHF protocol. It consists of decoder, command processing, state controller, cyclic redundancy check (CRC), random number generator (RNG), clock generator, encoder, power management, EEPROM access and sensor access. The data flow of the digital baseband can be divided into three major parts: receiving unit, controller unit and transmitting unit [34].

The receiving unit includes clock generator, decoder and command processing modules. The decoder module decodes the incoming Manchester-encoded data S_{dem} from RF/analog front-end, which is then processed in command processing module for other modules.

State controller, CRC, RNG, power management, EEPROM access and sensor access modules make up the controller unit. The state controller module is responsible for executing the actions including communicating with sensors and EEPROM, jumping to another state of operating procedure and collision arbitration. The CRC module calculates the CRC-16 for forward links and generates CRC-16 for return links to check data's integrality. The RNG is used to generate a one-bit true random number for collision arbitration. The EEPROM access module or sensor access module is employed to achieve the data communicating with EEPROM or sensor respectively. The power management module dynamically activates or deactivates the modules of digital baseband to effectively reduce its power dissipation.

4. Experimental Characterization

Fig. 9 shows the proposed self-powered RFID temperature sensor tag and the testing environment. To achieve the optimum communication performance, we adopt a dipole-like antenna design introduced in [23]. As for the energy harvest antenna, due to the antenna is close to metal, it should has good performance in avoiding metal interference. Thus we employ whip antenna as energy harvesting antenna. The proposed sensor tag chip was fabricated in TSMC 0.18 μm CMOS process. The packaged tag chip was assembled to a matched UHF antenna on FR4 substrate and the whole sensor tag covers around 85×52 mm^2. The VISN-R1200 is a special RFID tester from VI Service Network, which can process, analyze and display the testing signals simultaneously. The temperature performances of the sensor tag were measured in a climate chamber of Votsch VCL4003.

As shown in Fig. 10(a), detailed simulations taking into account the effect of the metal have been performed in HFSS by setting the minimization of the reflection

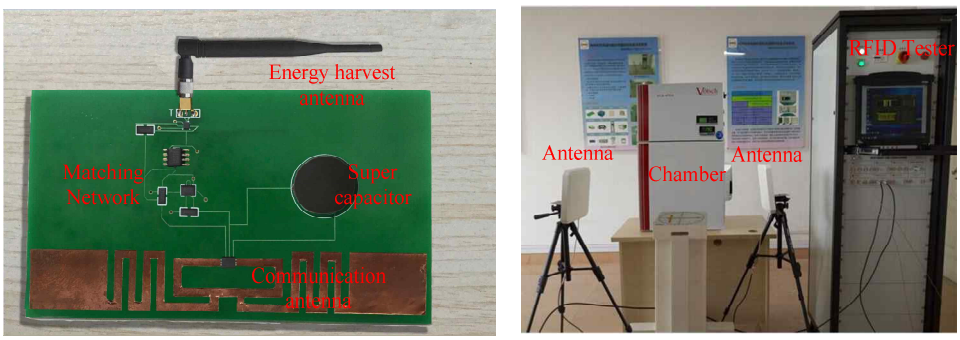

(a) (b)

Fig. 9. (a) The proposed RFID temperature sensor tag; (b) testing environment

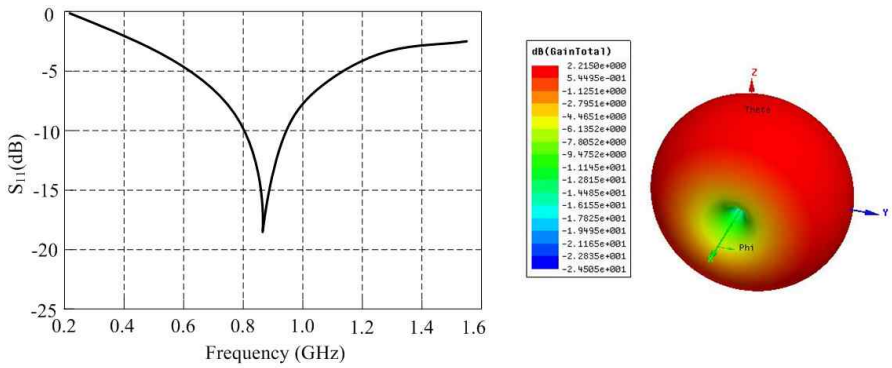

(a) (b)

Fig. 10. Parameters of the proposed antenna: (a) simulated S11; (b) radiation pattern

coefficient at the desired frequency (i.e.433 MHz) as the fitness function and by adopting a gradient-based interpolated quasi-Newton optimizer. For the energy harvesting antenna (433MHz), the radiation pattern is simulated, and for the communication antenna (915MHz), the S_{11} is simulated. It shows good performance of simulated S_{11}, confirming the proper antenna operation in the 433 MHz (-17 dB is the simulated S_{11}). The E-plane polar diagram in Fig. 10(b) depicts the typical radiation pattern achieved for the energy harvesting antenna (2.21 dB is the maximum realized gain), confirming the energy harvesting antenna has good performance in energy receiving.

To verify the RFID communication of the proposed temperature sensor tag, the testing parameters are chosen as following: the communication frequency is 915 MHz, the distances between the two antennas and the sensor tag are both 0.5 m, the transmitting power is 4 W. Then the overall communication flow is shown in Fig. 11. Firstly, the RFID tester sends Select instruction of Inventory Sequence order. After waiting for 5~6 Tari, the RFID tester sends Query instruction and the tag responses back with RN16. The tester then sends ACK instruction to acquire the EPC information of the tag including the sensor data. After that, the tester sends Req_RN instruction to obtain the Handle response.

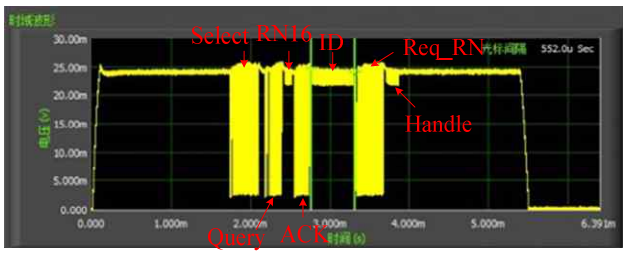

Fig. 11. The measured communication flow

The measured temperature performances of the sensor tag are shown in Fig. 12(a). The measurement is performed in chamber. The sensor tag was connected to the signal generator output for linearity testing. The sensor tag exhibits a linear behavior and a temperature resolution about 0.15 °C /LSB within the range from -20 ºC to 80 ºC. Temperature inaccuracy of the 5 test chips after 1-point calibration is shown in Fig. 12(b). The inaccuracy of the sensor is found to be -0.6/0.7 ºC (3σ) from -20 ºC to 80 ºC due to the process variation.

For a 100 MHz input frequency and 50 kΩ load, the η_r curve of the proposed rectifier is shown in Fig. 13(a). As compared to the conventional differential-drive rectifier [34], the proposed rectifier shows a flat η_r curve. When input power is 13 dBm, the two curves both reach the optimal point 69%. As for the input power range which η_r

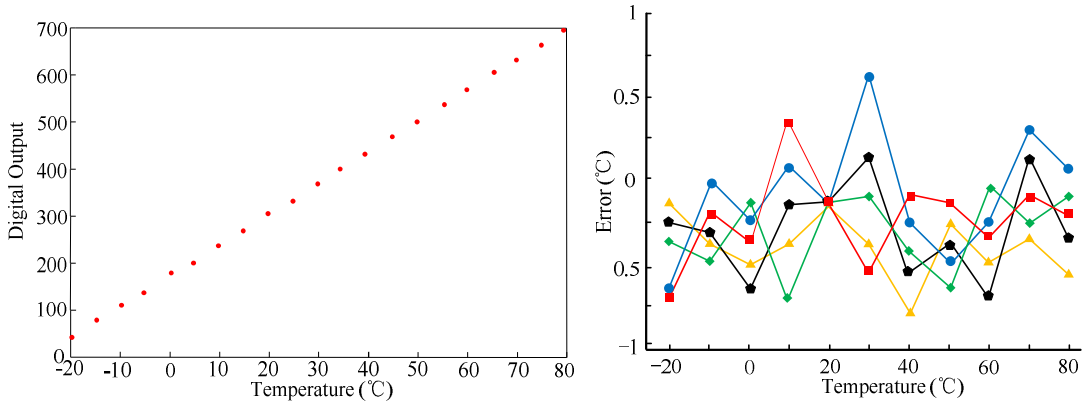

Fig. 12. Measured temperature performances: (a) linearity; (b) temperature error

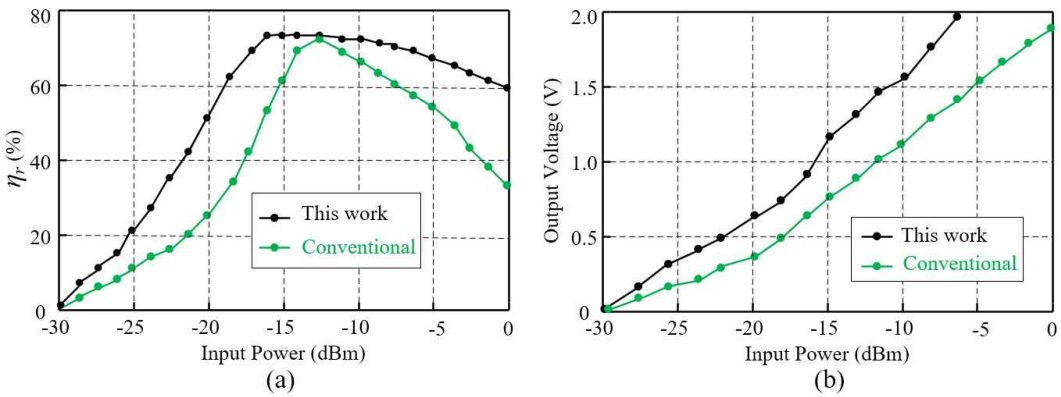

Fig. 13. Performance of the proposed rectifier: (a) power conversion efficiency and (b) output voltage

Table 1. Performances comparison of wireless temperature sensor

Reported Work	Process (μm)	V-Supply (V)	Error (℃)	Area (mm^2)	Resolution (℃/LSB)	Range (℃)	Power (μW)	Distance @EIRP (m)
This work	0.18	1.0	-0.6/0.7	0.35	0.15	-30~70	4.8	11.8@4W
[35]	0.13	1.0	±1.5	0.95	0.5	-40~85	No	7.2@4W
[36]	0.35	2.1	±0. 1	3.96	0.035	35~45	No	2@2W
[37]	0.18	1.2	±0.8	1.1	0.35	-20~30	32	4@4w
[38]	0.18	1.0	±1.5	0.73	0.5	-40~85	20	6@1W

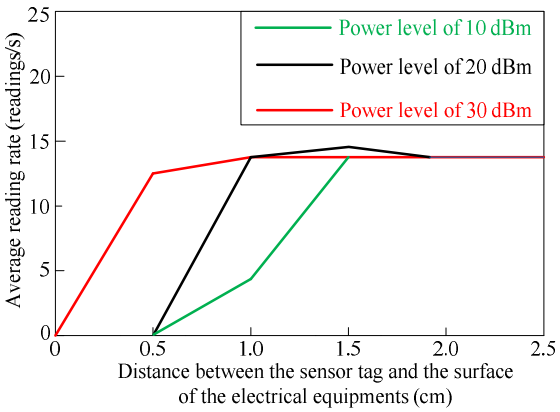

Fig. 14. Average read rate for different separation distances

is above 60%, the proposed rectifier and the conventional rectifier achieve −19 dBm and −7 dBm range, respectively. Fig. 13(b) compares the output voltage of the proposed rectifier with that of the conventional rectifier for a 50 kΩ load at 100 MHz input frequency. The proposed scheme provides an output voltage of 0.6 V at the low input power of −20 dBm, while this output for the conventional counterpart is 0.3 V which is insufficient for many RFID applications.

Table 1 compares the measured performances of the proposed design wither other wireless temperature sensor based on RFID technology. During the measurement of maximum operating distance, the wireless sensor was kept parallel with the antenna in the same height. The transmitting power of the transmitting antenna is 4 W. If the RFID tester can read the wireless sensor successfully 80 times over 100 attempts at one distance, we consider the wireless sensor can be read by tester successfully at this distance. Our design has a simple architecture and the measured minimum power dissipation is 4.8 μW, resulting in a maximum operating distance of 11.8 m under 4 W EIRP. Furthermore, due to the immunity to supply voltage variation, this work requires only 1-point calibration, ensuring low-cost applications

Performances of the self-powered RFID sensor tag mounted on different locations of the electrical equipments are experimentally evaluated, for the purpose of avoiding reading errors. All the experiments are carried out in a 110 kV outdoor substation. The distance between the sensor tag and the surface of the electrical equipments is increased at steps of 0.5 cm. Fig. 14 shows the measured

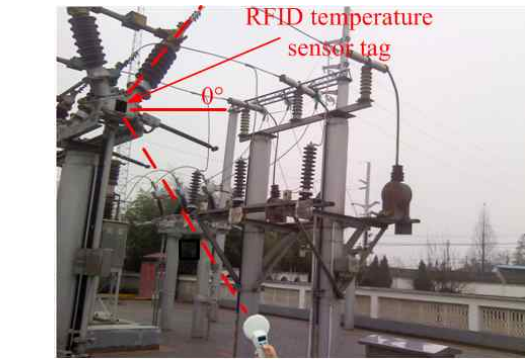

(a)

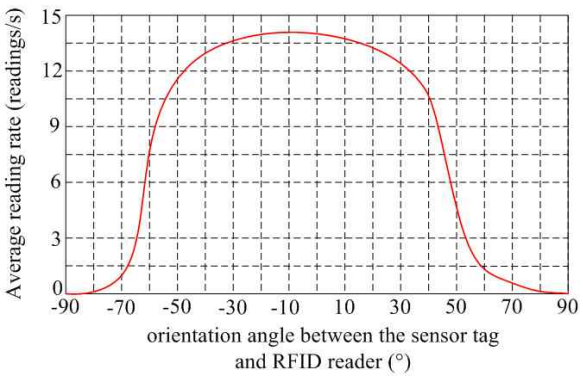

(b)

Fig. 15. Influence of orientation angle on data reading rate: (a) test environment, (b) measurement results

average reading rate in three different power levels: 10 dBm, 20 dBm and 30 dBm. When the sensor tag is directly attached on the surface of electrical equipments, the average reading rate is 0, resulting from the effect of eddy currents. When the power level is increased, the transmitted power intensity exceeds the electrical filed induced by eddy currents. Thus, from Fig. 14 it can be seen that with power level increasing, the minimum available distance decreases. When the distance is larger than 2 cm, there is no statistical difference in average reading rate. Considering the wireless transmission impedance matching and the analysis above, we employ a protective device made up of polymethylmethacrylate (PMMA) for the sensor tag. In this way, the interference can be effectively reduced to an acceptable level, and the sensor tag can operate on the electrical equipments reliably.

The influence of the orientation angle between the

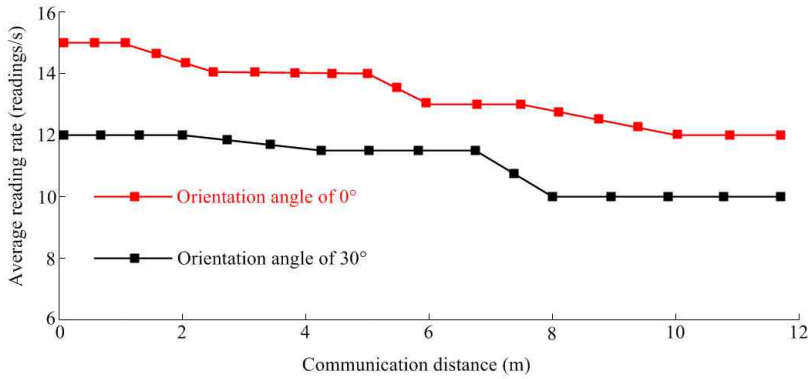

Fig. 16. Average reading rate vs. reader-tag distance

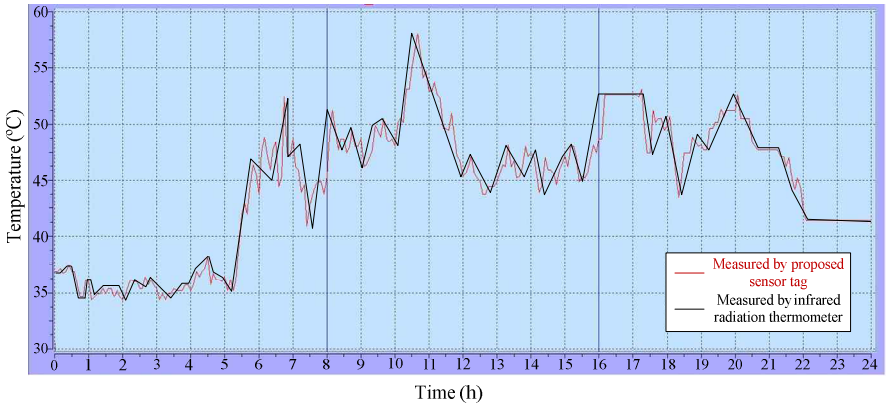

Fig. 17. Comparison of temperature measured in different methods

sensor tag and RFID reader on data transmission efficiency should also be studied. As is shown in Fig. 15(a), the sensor tag is mounted on the joint of the breaker, and a portable RFID reader is used to send instructions to the sensor tag and test the data reading rate, then the relationship between the angle of orientation and data reading rate is obtained. The results are shown in Fig. 15(b). From that it can be seen the maximum rate is achieved when the orientation angle is 0°, the average reading rate is 14 readings per second. With the orientation angle increasing to 60°, the average reading rate decreases to 7 readings per second. When the angle is larger than 75°, the rate is nearly 0. Hence, in order to achieve the optimum measurement performance, the angle of orientation should be as vertical as possible.

Except for the optimum orientation angle, the communication distance should also be investigated. The experiments are performed with the orientation angle of 0ºand 30º. Fig. 16 shows the data reading rate at different distances between the reader and the tag. From that we can see small changes in the read rate are presented for different communication distance. When the orientation angle is 0º, the minimum reading rate of 14 readings/s is achieved for communication distance within the range of 7m. As for long communication distance (>7m), the minimum reading rate can reach 13 readings/s. And when the orientation angle is 30º, it the reading rate can reach 10 readings/s for the long communication distance (>7m). Thus we can mounted the RFID reader and the sensor tag within the orientation angle range of 0º- 30º for optimum performance. The maximum available reading distance is 11.8 m within the orientation angle range of 0º- 30º.

To verify the accuracy and reliability of the proposed self-powered RFID temperature sensor tag, the sensor tag is mounted on the joint of a breaker (as is shown in Figure 15(a)) to measure the temperature, at the same time an infrared radiation thermometer is employed to measure the temperature of testing area as control group. At last we compare these two groups of measurement results to acquire the curve chart (shown in Fig. 17) and analyze the reliability of the proposed sensor tag. As is shown in Fig. 17, the two groups of measurement results show highly similarity, and the maximum difference between the two groups of measured temperature is 1.7 ºC, proving that the proposed RFID temperature sensor tag has excellent performance in high voltage equipments temperature monitoring.

5. Conclusion

This paper proposes a novel self-powered RFID sensor

tag with capabilities of temperature measuring, data storage, and wireless delivering, which is employed for long range, long term and large scale temperature monitoring of high voltage equipments in substation. The temperature sensor employs a novel phased-locked loop (PLL)-based architecture to achieve higher temperature accuracy. Then a two-stage rectifier adopts a dynamic bias-voltage generator to boost the effective gate-source voltage of the switches in differential-drive architecture, resulting in a flat power conversion efficiency curve. A regulator is also proposed for offering a stable voltage to the subsequent circuit. The sensor tag chip was fabricated in TSMC 0.18μm 1P6M CMOS process. The measurement results show that the proposed temperature sensor tag achieve a resolution of 0.15 °C /LSB and a temperature error of -0.6/0.7 °C within the range from -30 °C to 70 °C. The proposed sensor tag achieves maximum communication distance of 11.8 m.

Preliminary studies have shown promise in long-term temperature monitoring in substation, and future researches will focus on its performance in extra high voltage substation and underground substation.

Acknowledgements

This work was supported by Natural Science Foundation of China (51767006, 51607004), Key Research and Development Plan of Jiangxi Province (20161BBE50075, 20161BBE50076), Natural Science Foundation of Jiangxi Province (20171BAB206045), Science and Technology Project of Education Department of Jiangxi Province (GJJ160491).

References

[1] Hainan Long, Leyang Zhang, Jiao Pang, Caixia Li and Tierui Song, "Design of substation temperature monitoring system based on wireless sensor networks," *in Proceedings of the IEEE International Conference on Advanced Computer Control, Shenyang*, Shenyang, China, March 2010.

[2] Zhang Jun, Dai Wei, Huang Di, Zhang Sanfeng and Ji Yi, "Zigbee Enabled Remote Temperature Monitor System for High-Voltage Substations," *in Proceedings of the IEEE Conference on Engineering and Technology.* Xian, China, May 2012.

[3] Fang Miaoqi, Wan Jian, Xu Xianghua and Wu Guangrong, "System for temperature monitor in substation with ZigBee connectivity," *in Proceedings of the IEEE International Conference on Communication Technology.* Hangzhou, China, November 2008.

[4] Huang Xinbo, Li Xiaobo, Wang Yong and Fang Shouxian,"An online temperature monitoring system of substation based on Zigbee wireless network," *in Proceedings of the IEEE International Conference on Electrical and Control Engineering*, Yichang, China, September 2011.

[5] Wang Qishui, Shang Zhijun, Cui Shijie, Zhang Hongyu and Zeng Peng, "Research and Application of Wireless Temperature Monitoring for Transformer Substation," *in Proceedings of the 25th IEEE Conference on Chinese Control and Decision*. Guiyang, China, May 2013.

[6] Lu Huihui and Yuan Yuxiang,"Substation equipment temperature monitoring system design based on self-powered wireless temperature sensors," *in Proceedings of the2nd International Conference on Systems and Informatics.* Shanghai, China, November 2014.

[7] Huang Xinbo, Huang Biao and Wang Hongliang, "Design of com-positive on-line monitoring and fault diagnosis system for high-voltage switch cabinet," *in Proceedings of the IEEE International Conference on Electrical and Control Engineering*, Yichang, China, September 2011.

[8] Wang Weiqing, Zhang Lei and Zhang Weihua, "Temperature Monitoring System of Electric Apparatus Based on Optical Fiber Fluorescence," *in Proceedings of the Fifth International Conference on Intelligent Systems Design and Engineering Applications.* Hunan, China, June 2014.

[9] Degan Zhang, Xiang Wang and Xiaodong Song, "New Medical Image Fusion Approach with Coding Based on SCD in Wireless Sensor Network," *Journal of Electrical Engineering & Technology*, vol. 10, no. 6, pp. 2384-2392, Oct. 2015.

[10] Degan Zhang, Guang Li and Ke Zheng, "An energy-balanced routing method based on forward-aware factor for Wireless Sensor Networ," *IEEE Trans. Industrial Informatics*, vol.10, no.1, pp. 766-773, Oct. 2014.

[11] Degan Zhang, Ke Zheng and Ting Zhang, "A Novel Multicast Routing Method with Minimum Transmission for WSN of Cloud Computing Service," *Soft Computing*, vol.19, no.7, pp.1817-1827, July 2015.

[12] Degan Zhang and Yannan Zhu, "A new constructing approach for a weighted topology of wireless sensor networks based on local-world theory for the Internet of Things (IOT)," *Computers & Mathematics with Applications*, vol. 64, no. 5, pp. 1044-1055, Sept. 2012.

[13] Degan Zhang and Yanping Liang. "A kind of novel method of service-aware computing for uncertain mobile applications." *Mathematical and Computer Modelling*, vol. 57, no. 3-4, pp: 344-356, Feb. 2013.

[14] Degan Zhang, Ke Zheng and Dexin Zhao, "Novel Quick Start (QS) Method for Optimization of TCP," *Wireless Networks*, vol. 22, no. 1, pp. 211-222, Jan. 2016.

[15] Zhili Zhou, QM Jonathan Wu, Fang Huang and

Xingming Sun, "Fast and accurate near-duplicate image elimination for visual sensor networks," *International Journal of Distributed Sensor Networks*, vol. 13, no. 2, Feb. 2017.

[16] Zhang Degan, Zhao Chenpeng, Liang Yanpin and Liu Zhaojun, "A new medium access control protocol based on perceived data reliability and spatial correlation in wireless sensor network," *Computers & Electrical Engineering*. vol. 38, no. 3, pp. 694-702, May 2012.

[17] Wang Baowei, Gu Xiaodu, Li Ma and Yan Shuangshuang, "Temperature Error Correction based on BP Neural Network in Meteorological WSN," *International Journal of Sensor Networks*, vol. 23, no. 4, pp. 265-278, April 2017.

[18] Jian Shen, Shaohua Chang, Jun Shen, Qi Liu and Xingming Sun, "A lightweight multi-layer authentic-cation protocol for wireless body area networks," Future Generation Computer Systems, vol. 78, no. 3, pp. 956-963, Jan. 2018.

[19] Deng Fangming, He Yigang, Li Bin, Zuo Lei, Wu Xiang and Fu Zhihui, "A CMOS pressure sensor tag chip for passive wireless applications," *Sensors*, vol. 15, no. 3, pp. 6872-84, March 2015.

[20] Degan Zhang, Xiang Wang and Xiaodong Song, "A Novel Approach to Mapped Correlation of ID for RFID Anti-collision," *IEEE Trans. Services Computing*, vol.7, no. 4, pp. 741-748, Dec. 2014.

[21] Zhang Degan, Li Wenbin, "Novel ID based Anti-collision Approach for RFID," *Enterprise Information Systems*, vol. 10, no. 7, pp. 771-789, Jan. 2016.

[22] Danilo De Donno, Luca Catarinucci and Luciano Tarricone, "A Battery-Assisted Sensor-Enhanced RFID Tag Enabling Heterogeneous Wireless Sensor Networks," *IEEE Sensors Journal*, vol. 14, no. 4, pp. 1048-1055, Nov. 2014.

[23] Danilo De Donno, Luca Catarinucci and Luciano Tarricone, "Enabling self-powered autonomous wireless sensors with new-generation I^2C-RFID chips," *in Proceedings of the IEEE MTT-S International Conference on Microwave Symposium Digest (IMS)*, Seattle, USA, June 2013.

[24] Degan Zhang and Xiaodan Zhang, "Design and imple-mentation of embedded un-interruptible power supply system (EUPSS) for web-based mobile application," *Enterprise Information Systems*, vol. 6, no. 4, pp. 473-489, Oct. 2011.

[25] Tong Jin, He Yigang, Li Bin, Deng Fangming and Wang Tao, "A Novel Design of Radio Frequency Energy Relays on Power Transmission Lines," *Energies*, 2016, vol. 9, no. 6, pp. 476-486, Jun. 2016.

[26] Deng Fangming, He Yigang, Li Bing, Zhang Lihua, Wu Xiang, Fu Zhihui and Zuo Lei, "Design of an Embedded CMOS Temperature Sensor for Passive RFID Tag Chips," *Sensors*, 2014, vol. 15, no. 5, pp. 11442-11453, May 2015.

[27] Udo Karthaus and Martin Fischer, "Fully integrated passive UHF RFID transponder IC with 16.7-μW minimum RF input power," *IEEE Journal of Solid Sate Circuits Society*, vol. 38, no. 10, pp. 1602-1608, Sept. 2003.

[28] Raymond E. Barnett, Liu Jin and Steve Lazar, "A RF to DC Voltage Conversion Model for Multi-Stage Rectifiers in UHF RFID Transponders," *IEEE Journal of Solid Sate Circuits Society*, vol. 44, no.2, pp. 354-370, Jan. 2009.

[29] Paul T. Theilmann, Calogero D. Presti, Dylan Kelly and Peter M. Asbeck, "Near zero turn-on voltage high-efficiency UHF RFID rectifier in silicon-on-sapphire CMOS," *in Proceeding of the 2010 IEEE Radio Frequency Integrated Circuits Symposium (RFIC),* Anaheim, USA, May 2010.

[30] Hans Rabén, Johan Borg, Jonny Johansson, "An active MOS diode with Vth-cancellation for RFID rectifiers," *in Proceeding of the 2012 IEEE International Conference on RFID,* Orlando, USA, April 2012.

[31] Ka Nang Leung and Philip K. T. Mok, "A sub-1-V 15-ppm/℃ CMOS bandgap reference without requiring low threshold voltage device," *IEEE Journal of Solid-State Circuits*, vol. 37, no. 4, pp. 526-529, Aug. 2002.

[32] Luca Magnelli, Felice Crupi, Pasquale Corsonello, Calogero Pace and Giuseppe Iannaccone, "A 2.6 nW, 0.45 V Temperature-Compensated Subthreshold CMOS Voltage Reference," *IEEE Journal of Solid-State Circuits*, vol. 46, no. 2, pp. 465-474, Dec. 2011.

[33] Yang Xin, Huang Jinfeng, Feng Xiaoxin, Shen Jinpeng, Qi Yongzhen and Wang Xian, "Novel baseband processor for ultra-low-power passive UHF RFID transponder," *in Proceedings of the IEEE International Conference on RFID-technology & Applications*, Guangzhou, China , June 2010.

[34] Hannes Reinisch, Martin Wiessflecker, Stefan Gruber, Hartwig Unterassinger, Günter Hofer, Michael Klamminger, Wolfgang Pribyl and Gerald Holweg, "A multifrequency passive sensing tag with on-chip temperature sensor and off-chip sensor interface using EPC HF and UHF RFID technology," *IEEE Journal of Solid-State Circuits*, vol. 46, no. 12, pp. 3075-3088, Oct. 2011.

[35] Vaz, A., Ubarretxena, A., Zalbide, I., Pardo, D., Solar, H., Garcia-Alonso, A. and Berenguer, R., "Full passive UHF tag with a temperature sensor suitable for human body temperature monitoring," *IEEE Transaction on Circuits System II Express Briefs*, vol.57, no. 2, pp.95-99, Feb. 2010.

[36] Yin Jun, Yi Jun, Law Man Kay, Ling Yunxiao, Lee Man Chiu, Ng Kwok Ping, Gao Bo, Luong Howard C., Bermak Amine, Chan Mansun, Ki Wing-Huang, Tsui Chi-Ying and Yuen Matthew, "A system-on-chip EPC Gen-2 passive UHF RFID tag with embedded

temperature sensor," *IEEE Journal of Solid-State Circuits*, vol. 45, no.11, pp. 2404-2420, Oct. 2010.
[37] Qi Zengwei, Zhuang Yiqi, Li Xiaoming, Liu Weifeng, Du Yongqian and Wang Bo, "Full passive UHF RFID Tag with an ultra-low power, small area, high resolution temperature sensor suitable for environment monitoring," *Micro-electronics Journal*, vol. 45, no. 1, pp. 126-131, Jan. 2014.

Zhongbin Chen He received B.E. degree from Anhui Normal University in 2001 and M.E. degree in 2009 from East China Jiaotong University. He joined School of Electrical and Automation Engineering, East China Jiaotong University from 2002 and worked as a lecturer since 2004. His research interests include analog & mixed-signal circuit design, sensor processing and RFID technology.

Fangming Deng He received B.E. degree from Anhui Normal University in 2001 and M.E. degree in 2009 from East China Jiaotong University. He joined School of Electrical and Automation Engineering, East China Jiaotong University from 2002 and worked as a lecturer since 2004. His research interests include analog & mixed-signal circuit design, sensor processing and RFID technology.

Yigang He He received the M.Sc. degree in electrical engineering from Hunan University, Changsha, China, in 1992 and the Ph.D. degree in electrical engineering from Xi'an Jiaotong University, Xi'an, 2 China, in 1996. In 1990, he joined the College of Electrical and Information Engineering, Hunan University and was promoted to Associate Professor, Professor in 1996, 1999, respectively. From 2006 to 2011, he worked as the Director of the Institute of Testing Technology for Circuits and Systems, Hunan University. He was a Senior Visiting Scholar with the University of Hertfordshire, Hatfield, U.K., in 2002. In 2011, he joined the Hefei University of Technology, China, and currently works as the Head of School of Electrical Engineering and Automation, Hefei University of Technology. His teaching and research interests are in the areas of circuit theory and its applications, testing and fault diagnosis of analog and mixed-signal circuits, electrical signal detection, smart grid, radio frequency identification technology, and intelligent signal processing. He has published some 200 journal and conference papers in the aforementioned areas and several chapters in edited books.

Zhen Liang He received B.S. degree in mechanical and electrical engineering from the Qingdao University in 2000, and M.S. degree in electrical and computer engineering from Shandong University of Science and Technology in 2005. He is currently working toward the Ph.D. degree at the South China University of Technology, Guangzhou, China. Since July 2005, he worked at Rising Micro Electronics Co. Ltd, Guangzhou as an IC Design Engineer. His interests include designing analog RF and mixed-signal circuits for wireless communication system.

Zhihui Fu He received B.E. degree in 1999 in electronics engineering from Nanchang University, Nanchang, China and received M.E. degree in 2002 in electrical engineering from Chongqing University, Chongqing, China. He joined School of Electrical and Automation Engineering, East China Jiaotong University from 2002 and worked as a lecturer since 2004. His research interests include CMOS sensor technology, mix-signal circuit design and signal processing.

Chaolong Zhang He received the M.Sc. degree from Nanjing University of Information Science & Technology in 2008. He is currently an associate professor at School of Physics and Electronic Engineering, Anqing Normal University. He is also a doctoral candidate at School of Electrical Engineering and Automation, Hefei University of Technology. His current research interests include fault diagnostics and prognostics of analog and mixed-signal circuits, and battery capacity prognostic.